Thrust measurement using a plasma pressure probe immersed in the plume

Conference Paper · June 2022

CITATIONS
0

READS
89

4 authors, including:

Séverin Astruc
Office National d'Études et de Recherches Aérospatiales
3 PUBLICATIONS **77** CITATIONS
SEE PROFILE

Paul-Quentin Elias
Office National d'Études et de Recherches Aérospatiales
56 PUBLICATIONS **846** CITATIONS
SEE PROFILE

Thrust measurement using a plasma pressure probe immersed in the plume

IEPC-2022-414

Presented at the 37th International Electric Propulsion Conference
Massachusetts Institute of Technology, Cambridge, MA USA
June 19-23, 2022

Séverin Astruc[1] and Paul-Quentin Elias[2]
ONERA, Université Paris Saclay, F-91123 Palaiseau, France

Raphael Levy [3] and Vincent Gaudineau[4]
ONERA, Université Paris Saclay, F-92322 Châtillon, France

A probe is developed to measure the thrust of an electron cyclotron resonance thruster (ECRT). A controlled arm holds the probe in the plasma produced by the thruster. It is composed of two quartz micro-mechanical systems (MEMS) used as a pressure sensor. In addition to the plasma pressure, multiple perturbation forces such as the mechanical noise from the pump, electrostatic forces or neutral gas accumulation, affect the sensors. In this study, we show how the performance of the probe is increased against these perturbations and how we measure the pressure.

I. Introduction

The thrust in electric propulsion rarely exceeds the newton, even for the most powerful systems. The solution used to qualify an electric thruster during ground tests is the thrust balance [1]. This device is a pendulum fixed to the vacuum facility and supports the thruster. The deflection of the pendulum arm is linked to the thrust. Unfortunately, some ground tests like thermal cycling test cannot be performed with a balance. Moreover, most thrust balances are tailored-made for a given vacuum facility. This prevents straightforward performance comparison between facilities and the normalization of qualification tests.

An alternative to these balance measurements is to use a pressure probe immersed in the plume of the thruster, as shown in Fig. 1. The thrust is recovered by integrating the measurement over the plume section. In previous work, we demonstrated the feasibility of this measurement with a quartz micro-resonator (VIA) used as a pressure sensor [2]. Static tests showed that the sensor is sufficiently sensitive to measure the thrust, and the mechanical bias can be compensated by using two sensors in differential configuration. However, the sensor suffered from thermal transient and electrostatic effects. The sensor electronic was also perturbed when it was located in the densest place of the plume.

In this study, we choose a more sensitive and more optimized pressure sensor (ROSA) [3] designed and manufactured by ONERA, shown in Fig. 2. The better performances enable a lower sensor surface exposure to limit thermal and electrostatic effects. Additionally, to address the previous issues, a metal layer is deposited on the exposed face of the sensor to mitigate the charge deposition effect and enhance the heat diffusion over the sensor. Simulations of this design [4] show a decrease in the static thermal bias. A new sensor packaging is designed to provide better protection of the sensor as well as electrostatic shielding. This paper aims to determine the performance of this probe experimentally and retrieve the plasma pressure in the plume of the ONERA electron cyclotron resonance (ECR [5])

[1] severin.astruc@onera.fr.
[2] paul-quentin.elias@onera.fr
[3] raphael.levy@onera.fr
[4] vincent.gaudineau@onera.fr

electric thruster at a given position. Firstly, we briefly present the sensor's design along with its electronics and the improvement to be resilient against plasma exposure. Then, section III shows the experimental setup needed to measure the pressure at a given point for the ONERA 30W ECR thruster. Finally, we present the results and the performance of this thrust probe.

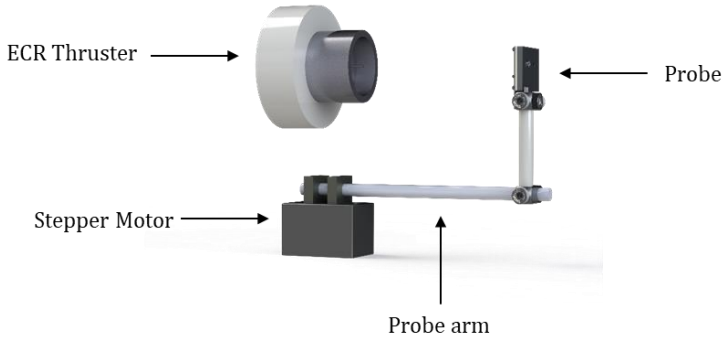

Fig. 1 Model of a thrust probe in front of the ONERA's electric thruster. An arm holds the probe and is mounted on a rotation stage (stepper motor) to perform angular scan of the plasma plume.

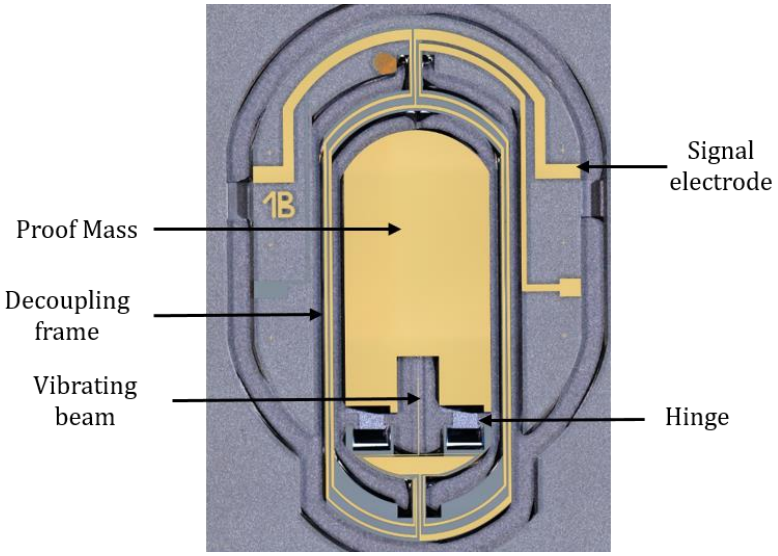

Fig. 2 Microscope photography of the quartz resonator. The beam oscillates in the plane, and its frequency is dependent of the pressure applied on the proof mass.

II. Probe design

A. Quartz sensor

The ROSA sensor is etched from a 500µm monolithic α-quartz wafer. It is composed of a proof mass linked to the sensor frame by hinges and a beam. The beam is actuated at resonance frequency through piezoelectric actuation by means of electrodes deposited on the beam surface. The design allows the proof mass to swing around the hinges when a pressure is applied at the front of the proof mass. This movement applies a strain on the beam and the frequency increases. On the contrary, a pressure at the rear face of the proof mass compresses the beam and thus decrease its frequency. Equation 1 shows the link between the pressure on the proof mass and the frequency of the beam.

$$f = f_0 + S_1 P + S_2 (P)^2 + \delta(T) \quad (1)$$

With f (Hz) the frequency of the beam, $f_0 \cong 50$kHz the frequency at rest, P ($\mu N.cm^{-2}$) the pressure applied on one face of the proof mass, $S_1 = 0{,}291\ Hz/(\mu N.cm^{-2})$ the linear sensitivity, $S_2 = -\frac{1}{2}\frac{S_1^2}{f_0}\ Hz/(\mu N.cm^{-2})^2$ [7] the quadratic sensitivity and $\delta(T)$ (Hz) the non-linear temperature induced frequency variation. The nonlinear sensitivity of order 3 and above have been ignored because of their small values.

With two sensors in differential configuration under the same pressure, as shown in Fig. 3, it is possible to reduce the nonlinear and the thermal effects. On the first sensor, the pressure is applied at the front face of the proof mass, thus it increases the frequency. On the second sensor, it is the rear face of the proof mass, which is under the same pressure. Here, the frequency decreases because the vibrating beam is compressed. Assuming the same frequency at rest for both sensors, opposite pressure $P_1 = -P_2$, same thermal drift and same sensitivity, then the frequency difference between the two sensors is linearly related to the applied pressure, see Eq. 2.

$$\Delta f = 2 S_1 P \quad (2)$$

This differential measurement rejects all common mode perturbation on the sensor: accelerations and forces affecting both proof masses. This method is important to decrease noise bias from the environment (vacuum pumps, motors, tilt of the sensor from gravity acceleration). The manufacturing process of the sensors limits the performance of this method. Indeed, each beam has slightly different dimensions that change the sensitivity and the performance of the sensor. It does not allow perfect compensation and in practice, there is a residual effect of the perturbations, although an order of magnitude lower than the uncompensated measurement.

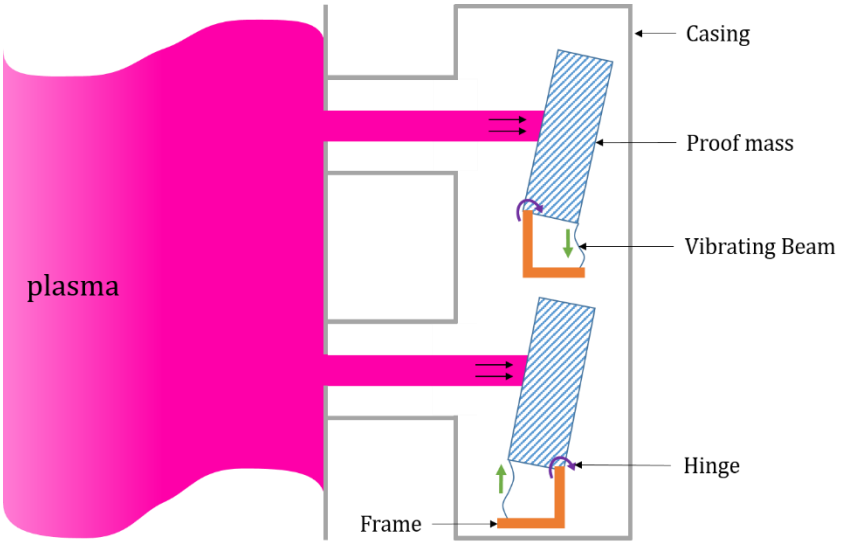

Fig. 3 Schematic view of differential thrust measurement. Two sensor cells are exposed to the plasma pressure. The proof mass displacement decreases the beam tension for the upper cell and increases the beam tension for the lower cell.

The sensor is subject to thermal frequency bias via plasma heating of the proof mass. There is two types of heating. First, the sensor temperature can increase at each point of the cell. This global rise of the temperature can be compensated by the knowledge of the cell temperature or the differential measurement. The other type of thermal frequency bias comes from the local difference of temperature as the quartz has poor conductive thermal transfer properties and the beam section surface is one order of magnitude less than the proof mass section, creating a thermal bottleneck. In this case, the differential measurement can remove this bias with the hypothesis that the local difference of temperature are the same in both cells. As it is not always the case, a solution is to deposit a gold electrode on the proof mass and the decoupling frame to homogenize the temperature around the beam, decreasing the local fluctuation of temperature and then the change in frequency. Additionally, it increases the conductive cooling, decreasing the

global temperature of the sensor. Previous works [4] shows a twenty fold reduction of the thermal drift with this electrode.

This sensor has better performance than the pressure sensor (VIA) used to demonstrate the feasibility, with the performance shown in table 1. The sensitivity of the sensor is increased by a factor thirty. This increases the precision of the pressure measurement and it enables to measure the pressure at wide angle from the thruster axial axis. Alternatively, this gain in sensitivity can be used to focus the plasma in the center of the proof mass thus decreasing the surface of collection and so the sensitivity of the measurement but it prevents the plasma particles from being collected by the electrodes on the cell and it decreases the heating of the cells.

Tab. 1 Performances of the VIA and ROSA cells used as pressure sensor

		VIA	ROSA
Sensitivity	$Hz/(\mu N.cm^{-2})$	0.012	0.291
Proof Masse surface area	cm^2	0.05	0.25
Bias stability (>3s)	$\mu N.cm^{-2}$	0.004	5.10^{-5}
Noise (@ 10Hz)	$\mu N.cm^{-2}$	0.001	10^{-4}
Bias repeatability [-40°C – 80°C] (after thermal compensation)	$\mu N.cm^{-2}$ rms	0.1	0.003
Scale factor repeatability [-40°C – 80°C] (after thermal compensation)	ppm rms	15	
Range	$\mu N.cm^{-2}$	10^5	5.10^3
Bandwidth	Hz	1000	

B. Probe

The plasma pressure probe is composed of two pressure sensors that measure differentially the pressure as shown in Fig. 4. The sensor with the front of the proof mass facing the plasma is named ‘top’ and the sensor impacted on the rear of the proof mass is named ‘bottom’. These sensors are soldered on a PCB board with the proximity electronics. This board is encapsulated by a packaging in aluminum. A plate with two apertures of 250µm in radius directs the plasma to the proof masses, as shown in Fig. 5. A shutter protects the sensors when needed. It is composed of a stepper motor and a protecting plate. It is used to estimate mechanical biases while removing the plasma pressure on the probe. In addition, it allows measuring the pressure with different time of exposure to the plasma. Finally, it protects the sensors from long exposure resulting in ion sputtering. When this shutter is open, the plasma hits the packaging, and the sensors. Charges are deposited and unwanted forces could appear. To avoid this, the packaging, the electronics and the sensors are maintained at the same potential. In this study, the potential is vacuum chamber ground. As the plasma impinges the sensors, the neutral gas pressure can increase in the probe internal volume. To avoid this, back-facing holes are located behind the sensors to evacuate the neutral gas and the plasma.

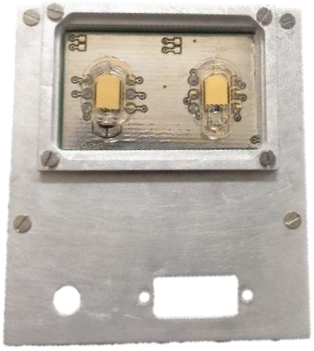

Fig. 4 Probe without the protection plate nor the shutter system. The two pressure sensors are mounted in an isopotential enclosure.

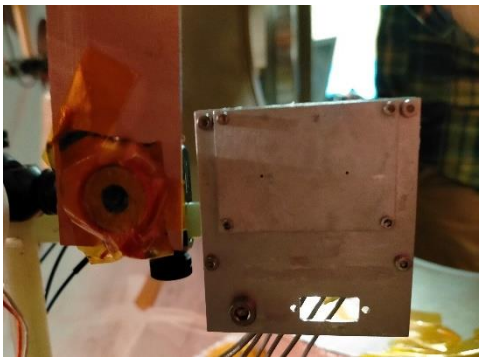

Fig. 5 Probe with the protection plate composed of two apertures (0.5 mm in diameter). A stepper motor can move the shutter in front of the two apertures

The accelerometer's beam is actuated with a sinusoidal signal. Thanks to the piezoelectric properties of the quartz and electrode design on the beam, the signal creates periodical mechanical stress on the beam. The closer the signal frequency is to the beam's natural frequency, the higher the displacement. The movement of the beam creates electric charges proportional to this displacement. A charge pre-amplifier collects the charges and provides a proportional voltage, as seen in Fig. 6. Outside of the probe, a phase-locked loop (PLL) gathers this sinusoidal signal and generates a feedback signal locked at the same frequency. This circuit constitutes an oscillator that follows the natural frequency of the beam. By monitoring the frequency of the beam, it is possible to deduce the pressure applied to the proof mass.

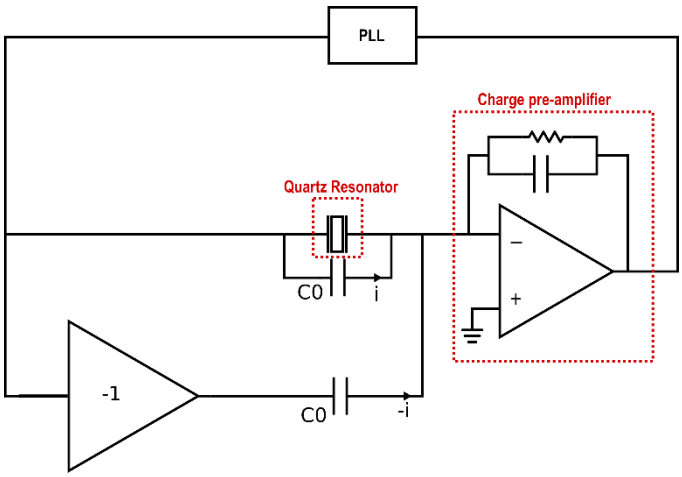

Fig. 6 Electric diagram of the oscillator electronic

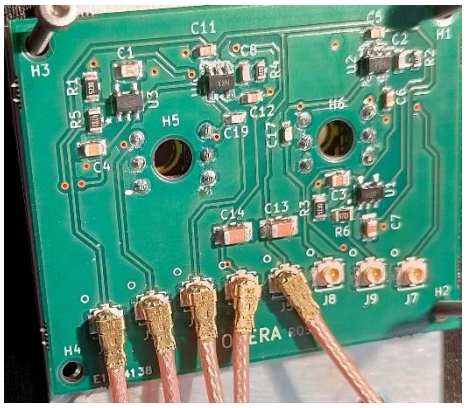

Fig. 7 Photo of the back face of the PCB board of the probe.

The beam's electrodes are close to each other and, then, forms a capacitor C_0 in parallel to the quartz resonator. Through this capacitor, the actuation signal creates a parasitic current *i* collected by the pre-amplifier. It is necessary to apply the opposite of the actuation signal on the same capacitance value to create a negative current *–i* between the beam and the charge pre-amplifier to compensate the parasitic current *i*.

III. Experiment setup

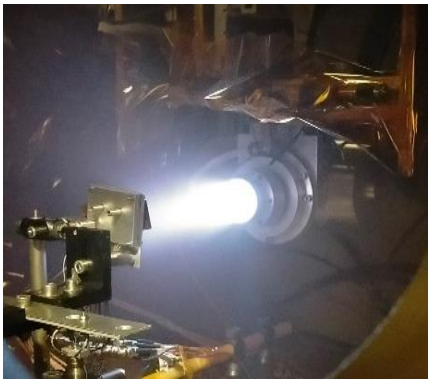

Fig. 8 The pressure measurement sensor is immersed into the plasma jet of the ONERA ECR thruster. An arm can move it with other diagnostic probes.

The whole setup is located at ONERA's B09 vacuum chamber (2m in length, 0.8m in radius). One primary pump, three turbomolecular pumps and one cryogenic pump achieve an ultimate background pressure of $5.10^{-7} mbar$. When the thruster is firing (0.1mg/s xenon), the background pressure reaches $10^{-5} mbar$.

The thruster used during the tests is an electron cyclotron resonance thruster developed by ONERA. It is composed of a coaxial chamber (27mm in diameter, 15mm in length [5]) with an antenna in its center. Xenon gas is injected at the back plate of this semi open cavity. A 2,45GHz electromagnetic wave is injected in the coaxial chamber and ionizes the gas. The plasma is then accelerated in a divergent magnetic nozzle produced by a permanent magnet. Further details can be found in [6].

During testing, the thruster was operated with a xenon flow rate of 0.1 mg/s and 30W injected power.

The plasma pressure experimental setup is composed of the probe mounted on a rotating arm in front of the thruster, as shown in Fig 8. The proof masses are located 29cm away from the backplate of the thruster. The probe can move from -40° to 40° around the axial axis. A faraday probe was placed at the same distance on the arm to obtain an angular profile of ion current density. By hypothesis, the beam is considered axisymmetric and composed by only single ionized xenon ions.

The thrust measurement is obtained by integrating the pressure produced by the thruster plasma over a plume section. By assuming an axisymmetric pressure, an angular scan around the axis is enough to retrieve the thrust. At each angle, a shutter is placed in front of the sensors to protect them against the plasma. The frequency given by the sensors depends of their initial frequency, their thermal and aging drift and their positional drift due to tilt from gravitational vector. By opening the shutter, the plasma pressure create a step in the frequency and after, a thermal drift slowly increase the frequency. Knowing the sensors sensitivity S_1, this frequency step can be converted to the equivalent pressure value.

IV. Results

A. Thruster parameters

The faraday probe gives the ionic density current J (A/m²) for these parameters in Fig. 9. At a given angle from the thruster axis, the current density is proportional to the xenon flux $\frac{J(\theta)}{q}$. As the xenon ion velocity is $v_{Xe} = 16km/s$ (measured from an ion energy analyzer) with a mass m_{Xe}, it results in a pressure:

$$P(\theta) = \frac{J(\theta)}{q} m_{Xe} v_{Xe} (\mu N.cm^{-2}) \quad (3)$$

This pressure applies a force on the proof mass according to the aperture size of the plate protecting the sensors, which creates a drift in the sensor frequency from the frequency with no thrust. The figure 9 gives the estimated pressure for specific angles and the corresponding frequency drift calculated from the faraday probe measurement. It is computed with an aperture diameter of 0.5mm and a sensitivity of the sensors of 0.291 Hz/µN.cm^{-2}.

The frequency drift varies from 0.1mHz to 3mHz. These values are well above the noise floor of the sensor by 3 decades in the worst case (high angle). At maximum, the aperture of the protecting plate could be 2.5mm. With this diameter size, the frequency can vary from 1mHz to 100mHz.

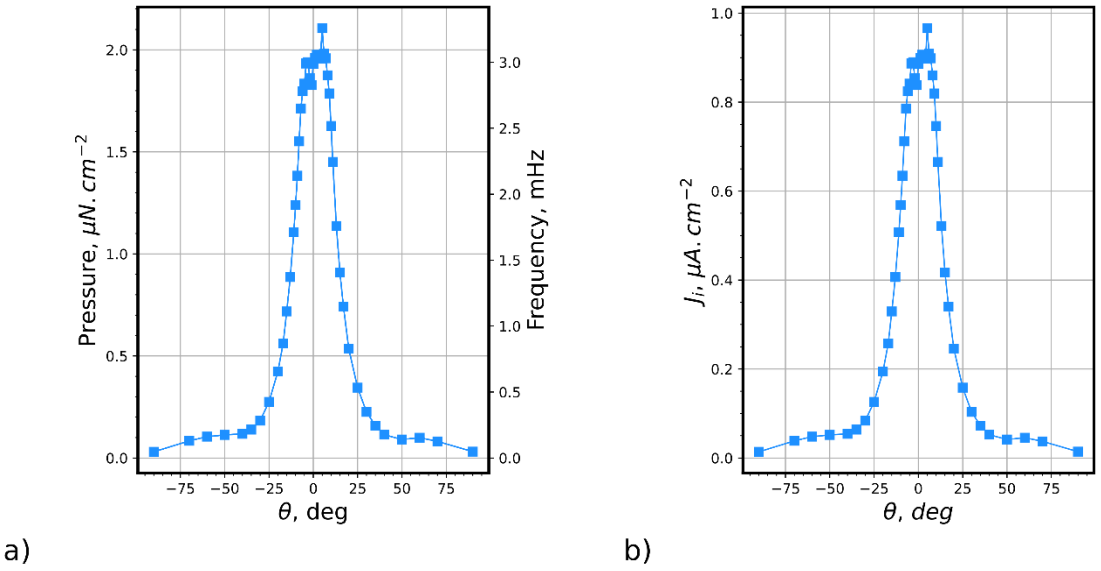

Fig. 9 a) Estimated plasma pressure with the ROSA sensor frequency drift associated at 29cm from the thruster at different angles. b) Faraday probe output for angular scan of the ion current density of the ECR thruster at 29cm from the thruster backplate

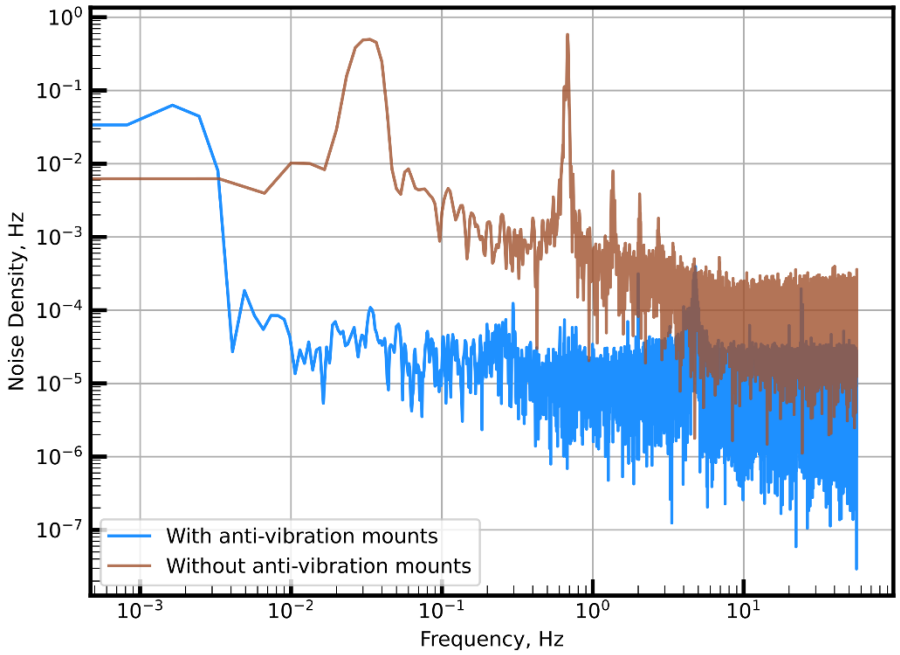

Fig. 10 Noise density spectrum of the sensors when all pumps of the vacuum tank are working. In blue, the spectrum when the stepper motor, holding the arm and the sensors, is mounted on anti-vibration mounts. In brown, there is no anti-vibration mounts.

B. Noise canceling

Initially, without operating the thruster, the frequency of the pressure sensors was not stable. The variation of signal frequency was around 1Hz. It was well above the expected frequency shift from the applied thruster pressure. It is also different in amplitude and frequency between the two sensors. In this case, the pressure measurement could not be feasible with or without differential measurement. The origin of this instability is the environment mechanical noise. When the arm holds the probe, it transmits the vibration from the vacuum facility pumps and the rotation stage.

The turbomolecular pump rotation speed is set to 525Hz with a resolution of 1Hz. The difference of speed between the three pumps creates a beat that is transmitted to the sensors. The figure 10 shows a frequency analysis of the signal where we can see three frequencies at 60 mHz, 1.5 Hz and 2Hz. These frequencies are responsible of the majority of the noise. The PLL setup includes a low pass filter with a 1Hz cutoff frequency. Lowering this frequency can filter the peak frequency of 0.6Hz but the response time of the system increases greatly and become not practical when we try to create a step change of frequency with the shutter. Another way to filter these frequencies is to implement a mechanical filter. It is not possible to achieve 1Hz cutoff frequency with a spring-like system between the arm and the probe because of the low weight of the probe (50g). A solution is to put the metallic frame holding the stepper motor, the arm and the probe (~4kg) on anti-vibration mounts. This design filters efficiently the beat frequency. It remains a very low frequency drift ($< 3.10^{-3}Hz$) which is inherent with the micro mechanical sensors. It is not a problem because, with the shutter, the interesting measuring time is around one second and below. For a measure integrated over one second, the noise is then $4 \times 10^{-4}Hz$.

C. Measurement in the plume

When the probe is exposed to the plasma with an open shutter and close to the thrust axis, the output signal is unstable with high frequency change (>10Hz), see Fig. 11. This high variation in signal is due to signal electrodes, on the sensors decoupling frame and on the vibrating beam, collecting charged particles directly after collisions or after secondary emissions. It explains why the top sensor is more sensitive to this instability as its signal electrodes faces the plasma.

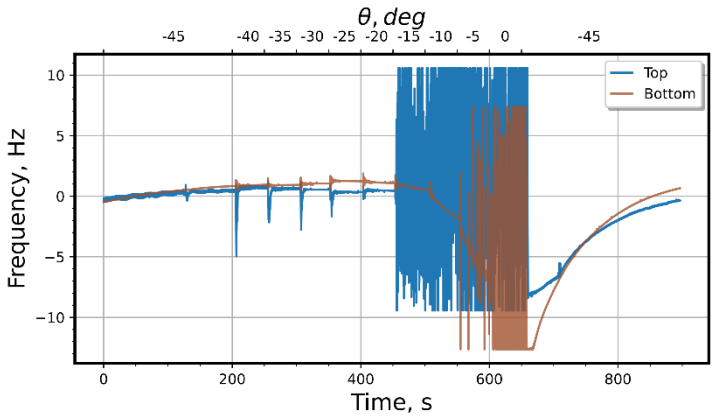

Fig. 11 Angular scan with the pressure sensors from $\theta = -45°$ to 0°. When the sensors are close to the thruster axis, the signal becomes unstable and it is not exploitable

To decrease the direct electrode collection, the aperture in the plate protecting the sensor needs to be small enough to avoid charged particles reaching the electrodes, as shown in Fig. 12. As the distance between the sensor surface and the plate is l=0.6mm, the thickness of the plate is e=0.2mm and the distance between the nearest signal electrode and the center of the proof mass is d=2.4mm, then the maximal aperture diameter is $a_{max} = \frac{d}{\frac{1}{2}\frac{l}{e}} = 0.69mm$.

The current resolution of the probe is $10^{-4}Hz$ given by the noise floor of the frequency analysis. The lowest estimated frequency shift from applied pressure is the same frequency. It was computed with an aperture diameter of $a_{min} = 0.5mm$. Hence, this is the minimal diameter aperture.

Finally, a tube of 16mm in length is mounted on the front cover. The tube inlet has a 0.5mm aperture to limit the plasma flow. The tube increases the e factor and then decreases the direct collection of charged particles. After these changes in the packaging, instabilities disappeared even in the thruster axis.

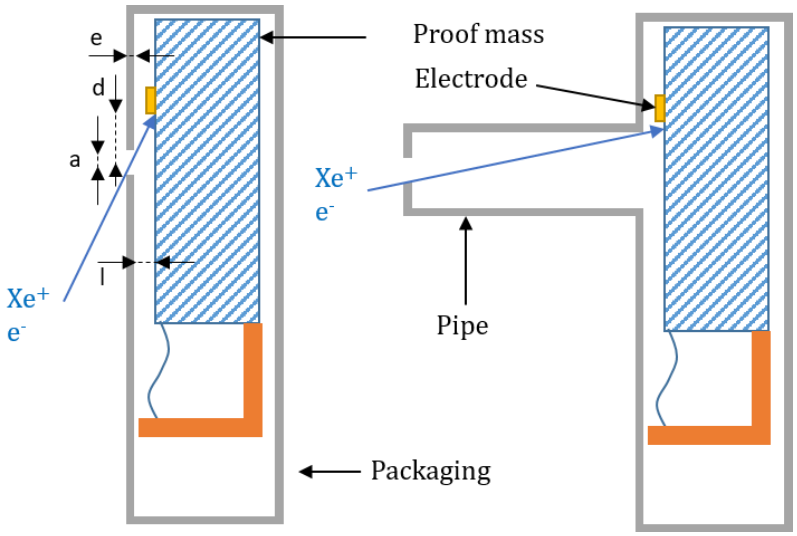

Fig. 12 Diagram of the sensor located in the packaging with the trajectory of charged particle. To the left, there is a simple aperture and to the right, a tube is added to lead the particles to the proof mass with a quasi-normal angle

D. Plasma pressure in the thruster axis

Now the probe is located in the thrust axis. The shutter is completely decoupled from the probe arm by fixing it to the vacuum tank. This design cancels all frequency drifts from the shutter operating but it does not allow an angular scan. The probe remains in the thrust axis. The figure 14 shows four successive openings and closings of the shutter. Both sensors experience change in frequency when exposed. These changes in frequency are in the same direction as predicted, increasing frequency for the top sensor and decreasing frequency for the bottom sensor. However, the absolute value of these changes $\Delta f = 480 \pm 43\ mHz$ is several orders of magnitude higher than the expected value. It is equivalent to $\Delta P = 310 \pm 31 \mu N/cm^2$. Additionally, the bottom sensor is experiencing a frequency shift three times higher than the top sensor.

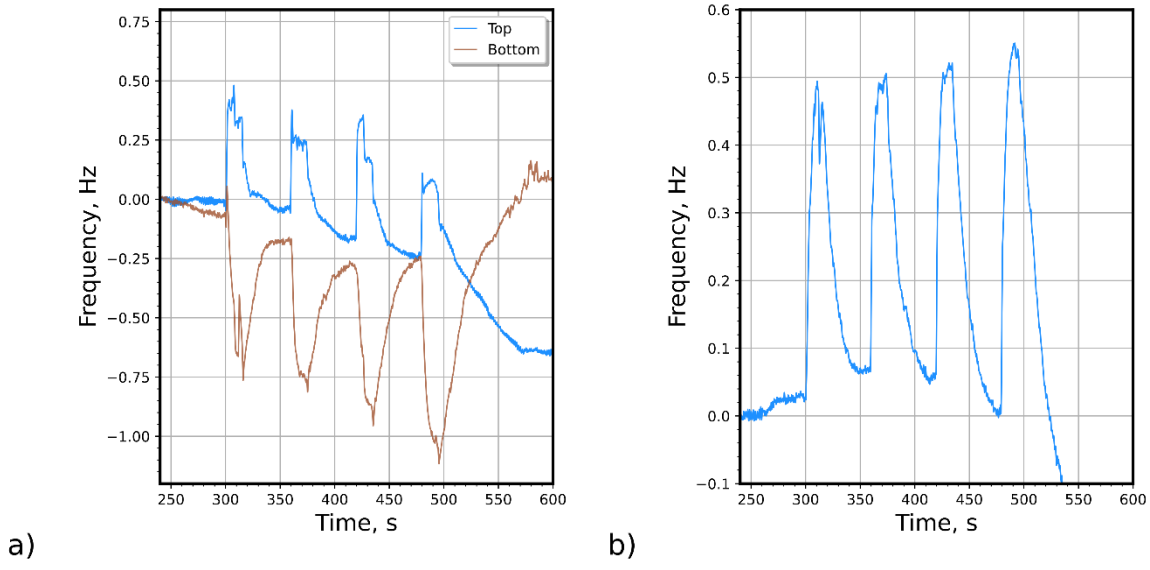

Fig. 14 Frequency change of the two sensors when the shutter is opened at minutes 5, 6, 7 and 8 for 15s each time. The a) figure shows the frequency of the top and bottom sensors. The b) figure shows the differential measurement obtained from Eq. 2.

V.Discussion & perspectives

We used two quartz MEMS as pressure sensors to examine the feasibility of a thrust measurement all over the plasma jet. The following results were found:

- These sensors were more sensitive by a factor 30 than those of previous work. With this sensitivity, the sensors measure the vibration from the vacuum pump. Anti-vibration mounts filtered effectively this perturbation.
- An angular scan shows that if the protection plate aperture is too big, signal electrodes collect a large portion of charged particles, perturbing the measurement. This collection was more important for the sensor 'top'.
- The great sensitivity of the sensor allowed decreasing the exposed surface of the sensors. A tube and a diaphragm reduced the collection of charged particle from signal electrodes.
- Finally, when the shutter was opened, a frequency shift was observed. However, its value was too high to correspond to the expected plasma pressure.

Two hypothesis have been emitted to explain why the frequency shift value does not correspond to the estimated frequency shift. The first hypothesis to explain this behavior is that there is an electrostatic force between the proof mass and the packaging. It was verified that each part of the packaging is grounded to the earth and there is no dielectric material in the vicinity of the sensors. Xenon ions sputter the metallic layer on the proof masses. Visually, there is no hole in the layer but black stains. There is no evidence of conductivity in these stains. Furthermore, it is not possible to verify that the metallic layer is still grounded. In all cases, electrostatic charges can accumulate and build up an electrostatic force. If we approximate the system by a two plates condenser, then the force is described by the Eq. 3.

$$F_{ES} = \frac{\varepsilon_0 S U^2}{2l^2} \tag{3}$$

With S the proof mass surface and U the voltage difference between the proof mass and the packaging. A voltage as low as 10V creates a force of 30nN which translates in a frequency drift of 0.5Hz.

The second hypothesis is the increase of the pressure in the sensor cavity. As the plasma enters the cavity, the pressure in front of the sensors increases while the pressure behind the sensor remains low. The low conductance between the cavity in front of the probe and the exhaust apertures on the back of the probe can sustain, in principle, a significant pressure difference. The sensitivity of the sensor is 0.291Hz/(µN.cm^{-2}) which means that a 0.5Hz drift correspond to a $2\mu N.cm^{-2} = 10^{-4} mbar$ pressure difference between the whole surface of the front and the rear face of the proof mass. To test if this hypothesis is valid, it is possible to modify the packaging to allow the gas to escape from the side near the sensors.

In both hypotheses, the local difference in the pressure or the voltage difference could result in a difference perturbation for both sensors.

VI.Conclusion

In this study, we used pressure sensors in differential configuration to estimate the plasma pressure produced by an ECR thruster. By integrating the measure over the plasma plume, this probe could give the thrust of an electric thruster without being mechanically linked as the thrust pendulums. These sensors are more sensitive than those used in previous work. As a consequence, they are more sensitive to the vibration noise from the vacuum pumps. The use of anti-vibration dumper allowed filtering this noise. A tube was added in front of both sensors to get the pressure produced by the particles normal to the sensor and so, reduce the unwanted particles collected by unprotected electrodes. Finally, a measure of the pressure in the thruster axis give results two orders of magnitude above the expected results. This suggests that unwanted perturbations are still influencing the pressure measure. It could be local pressure difference or electrostatic force. Future research will focus on finding the origins of these perturbations, and the means to suppress them.

Acknowledgments

This work has been co-funded by the CNES under the contract 51/19132. The authors would thank Alberto Rossi from CNES for his help.

References

[1] J. E. Polk *et al.*, "Recommended Practice for Thrust Measurement in Electric Propulsion Testing," *J. Propuls. Power*, vol. 33, no. 3, pp. 539–555, May 2017, doi: 10.2514/1.B35564.

[2] P.-Q. Elias, R. Levy, J. Jarrige, V. Gaudineau, and C. Boniface, "Thrust measurements using plasma pressure measurements in the plume a feasibility," presented at the IEPC2019.

[3] R. Levy, D. Janiaud, J. Guerard, R. Taibi, and O. L. Traon, "A 50 nano-g resolution quartz Vibrating Beam Accelerometer," in *2014 International Symposium on Inertial Sensors and Systems (ISISS)*, Laguna Beach, CA, USA, Feb. 2014, pp. 1–4. doi: 10.1109/ISISS.2014.6782532.

[4] S. Astruc, P.-Q. Elias, and R. Levy, "COMPENSATION OF PERTURBATIVE EFFECTS ON A THRUST MEASUREMENT MEMS PROBE FOR ELECTRIC PROPULSION," in *2021 Symposium on Design, Test, Integration & Packaging of MEMS and MOEMS (DTIP)*, Paris, France, Aug. 2021, pp. 01–06. doi: 10.1109/DTIP54218.2021.9568665.

[5] T. Vialis, J. Jarrige, A. Aanesland, and D. Packan, "Direct Thrust Measurement of an Electron Cyclotron Resonance Plasma Thruster," *J. Propuls. Power*, vol. 34, no. 5, pp. 1323–1333, Sep. 2018, doi: 10.2514/1.B37036.

[6] S. Peterschmitt, "Development of a stable and efficient electron cyclotron resonance thruster with magnetic nozzle," Institut Polytechnique de Paris.

[7] B. Le Foulgoc, "Evaluation du potentiel de performance de micro-accéléromètres inertiels vibrants en silicium," 2008.